JOURNAL OF MATERIALS SCIENCE **34** (1999) 5677–5680

Crystal defect generation during diffusionless transformations of boron nitride by puckering mechanism

V. F. BRITUN, A. V. KURDYUMOV
Institute for Problems of Materials Science, National Academy of Sciences of Ukraine, Kiev

The fine structure of wurtzitic and zincblende BN phases formed during diffusionless transformations by the puckering mechanism was investigated by X-ray diffraction and transmission electron microscopy. The formation of inversion boundaries in prismatic planes of wurtzitic BN was detected. Their appearance is directly connected with the puckering mechanism of transformation. Unlike these defects, the formation of faults in the zincblende phase is a result of plastic deformation which accompanies the diffusionless transformation.

1. Introduction

Under high pressure the graphite-like modifications of BN (hexagonal—hBN and rhombohedral—rBN) are transformed into dense phases with a tetrahedral coordination of atoms: wurtzitic—wBN (hexagonal 2H structure) or zincblende—zBN (cubic 3C structure) [1, 2]. The diffusionless (martensitic-type) mechanisms of transformation take place in the case when the initial hBN or rBN crystals have a high-ordered structure and the pressure is significantly higher than the pressure of equilibrium between the graphite-like and diamond-like phases [3, 4]. One of such mechanisms is that of basal layers puckering. It consists in splitting of the (0 0 0 1) planes of the graphite-like phase into two sublayers by means of B and N atoms displacements in opposite directions along the "*c*" axis. The hBN (or rBN) lattice compression and splitting of basal planes leads to strong chemical bond formation between the (0 0 0 1) planes, and the appearance a tetrahedral coordination of atoms. It has been shown experimentally that the puckering mechanism takes place in the cases of hBN → wBN and rBN → zBN transitions [5, 6].

There is a lot of work in which the real structure of wBN has been investigated by using X-ray diffraction and electron microscopy [7–9]. In all these works, high defect densities in wBN crystals were detected. That was explained by martensitic character of hBN → wBN transformation and metastability of wurtzitic phase. However the mechanisms of defect generation during martensitic transition has not been discussed. It has been found that the intrinsic stacking faults in wBN are formed during subsequent p, T treatment, and the concentration of these faults increases considerably just before wBN → zBN transformation ($p > 6$ GPa, $T > 1200\,^{\circ}$C) [9, 10].

Data concerning the zBN real structure formed during rBN → zBN transition by the puckering mechanism are absent in the literature. This paper reports the results of a study of wBN and zBN fine structure, formed by puckering mechanism.

2. Experimental procedure

Commercial hBN powder and CVD rBN plates were used as starting materials. The mean size of the plate-like particles of the hBN powder was about 5 μm (in the basal plane). The rBN plates had an axial texture, which had been described earlier in [11]. The hBN powder was compacted under low static pressure, and such samples were compressed by shock waves in cylindrical containers by the scheme of sliding detonation [12]. The maximum pressure in such scheme of loading did not exceed 20 GPa. The plane shock wave scheme (with pressures up to 60 GPa) was used for rBN compression, because the rBN → dense phase transition was not detected under pressures less than 20 GPa [6]. A part of the heterophase wBN + hBN compacts after shock wave loading was cleared from the hBN phase and compressed under hydrostatic conditions ($p = 7, 7$ GPa, $T = 1300$–$1400\,^{\circ}$C). These conditions correspond to the beginning of the wBN → zBN transformation.

The real structure of BN compacts after high pressure treatment was studied using X-ray diffractometer HZG-4 CARL ZEISS and electron microscop PEM-U SELMI. The thin samples for transmission electron microscopy were prepared by ionmilling.

3. Results and discussion

According to X-ray studies, after shock wave loading of hBN the heterophase compacts contained up to 60% wBN. The shock compression of rBN plates by flat waves led to the formation of 40% zBN. In both cases the puckering mechanism resulted in an characteristic orientational relationship between the phases:

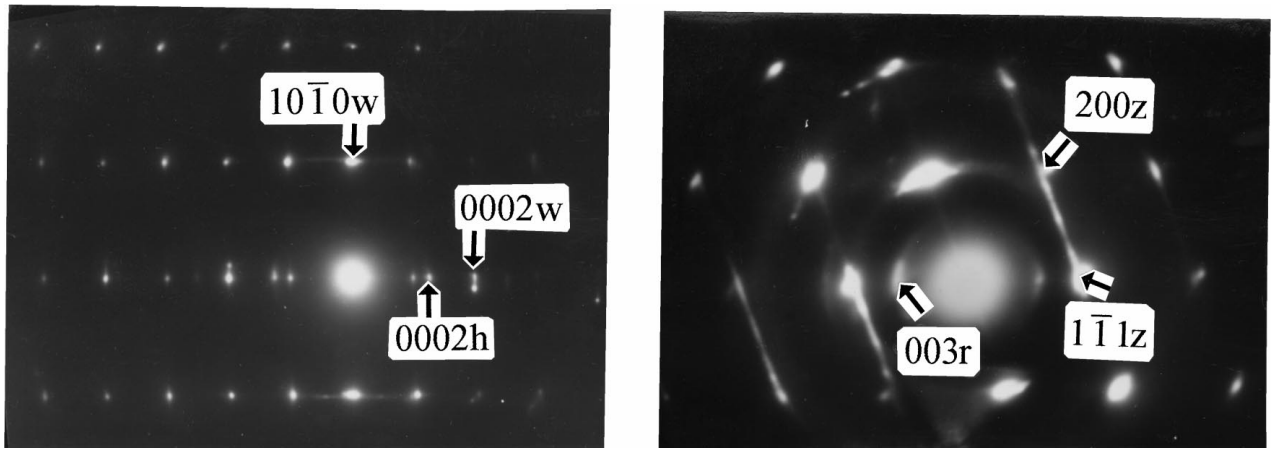

(a) (b)

Figure 1 SAD patterns from heterophase grains: (a) -hBN + wBN, axis zone [$\bar{2}$1 1 0]; (b) -rBN + zBN, axis zone [1 1 0]z.

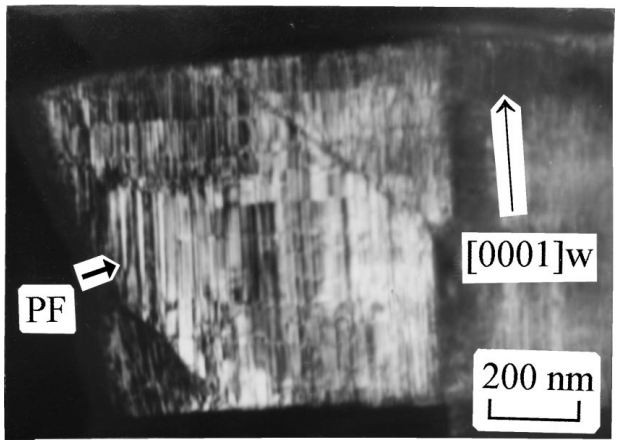

Figure 2 Prismatic faults (PF) in wBN, dark-field image, $g = 1\,0\,\bar{1}\,3$.

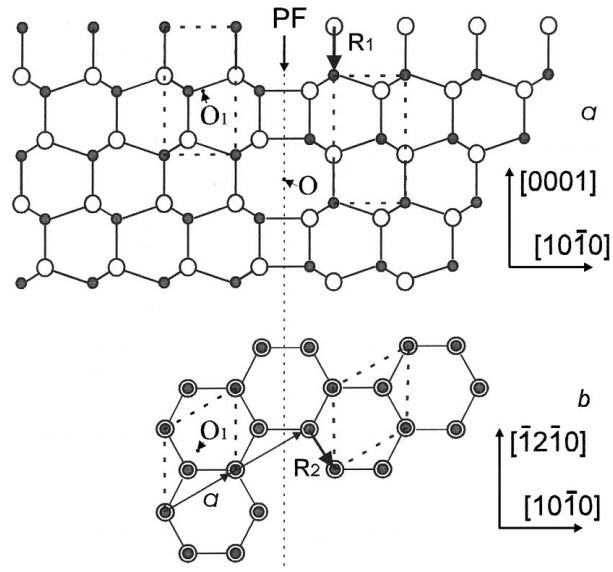

Figure 3 Scheme of prismatic fault: (a) projection on (1 1 $\bar{2}$ 0) plane; (b) projection on (0 0 0 1) plane.

(0 0 0 1)w||(0 0 0 1)h, [1 0 $\bar{1}$ 0]w||[1 0 $\bar{1}$ 0]h;

(1 1 1)z||(0 0 0 1)r, [1 1 $\bar{2}$]z||[1 0 $\bar{1}$ 0]r.

These orientational relationships were observed in selected area diffraction (SAD) patterns from heterophase particles with a axis zone [2 $\underline{1}$ $\underline{1}$ 0] (Fig. 1).

Electron micrographs of {$\bar{2}$ 1 1 0} wBN grain cross sections show striations due to flat faults in the prismatic {1 0 $\bar{1}$ 0} planes (Fig. 2). The density of such prismatic faults (PF) in some grains is much higher than the density of basal stacking faults. The bright-field contrast of the PFs is usually very weak. We observed good contrast only in dark-field image taken under the two-beam conditions for the following diffraction vectors ***g***: $\underline{0}$ 0 0 2, 1 0 $\underline{1}$ 2, 1 0 $\underline{1}$ 3. PFs were invisible if $g =$ 1 0 $\underline{1}$ 1. The PF contrast peculiarities don't correspond with any stacking faults (either basal, or prismatic) contrast described for different crystals with wurtzitic structure [13–15].

Analysis of BN atom displacements during puckering makes it possible to propose the following scheme of PF formation. If a large number of nuclei of wBN appear in the hBN single crystalline grain under coherent nucleation, the structure of nuclei can differ with respect to the atomic arrangement. These differences are connected with two variants of B and N atom displacement during (0 0 0 1) hBN planes splitting. In the first variant B atoms are displaced in [0 0 0 1] and N atoms in [0 0 0 1] directions. In the second variant the directions of atom displacements are opposite to the above mentioned. If different variants are realized in neighboring wBN nuclei then the prismatic fault must appear between these nuclei after their coalescence. The scheme of such defect is shown in Fig. 3. In the above scheme the PF is situated in the (1 0 $\bar{1}$ 0) wBN plane. Various schemes for different PF locations are possible, but experimental results show that the PFs are located just in {1 0 $\bar{1}$ 0} plane. As it can be seen from the scheme (Fig. 3) if PF is a boundary between two nuclei (A and B), then the crystal lattice of the first nucleus will be matched to the lattice of the second nucleus by inversion with point O as an inversion center. Thus we can identify the prismatic faults as inversional boundaries (IB) (in accordance with the terminology accepted in [16]). To explain the nature of the PF contrast it is convenient to take an O1 point as an inversion center (O1 is located in the center of the unit cell which is marked by dotted line in Fig. 3). Then two operations are necessary for A and B lattices matching: invertion relative to the O1 point, and displacement by the vector

R (which consists of the two components: $R1$ along the "c" axis, and $R2$ normal to "c", Fig. 3). In first approximation, $R = \frac{3}{8}[0\,0\,0\,1] + \frac{1}{3}[1\,0\,\bar{1}\,0] = \frac{1}{24}[8\,0\,\bar{8}\,9]$. The electron diffraction theory [17] shows that the planar fault contrast vanishes only when the product gR is an integer (R is displacement vector). The product gR is not integer for $g = 0\,0\,0\,2$, $1\,0\,\bar{1}\,2$, $1\,0\,\bar{1}\,3$ and for this reason PFs are visible in these diffraction conditions. The contrast of PFs vanishes if $g = 1\,0\,\bar{1}\,1$. In this case the product $gR = 25/24 \approx 1{,}04$ i.e. it differs slightly with respect to integer. We can propose that real vector of displacement R^* is some smaller than vector R found above, and then for real vector $gR^* = 1$. It may be connected with the decrease in the B—N bond length across the fault plane. The contrast of inversion domains is connected with a failure of Friedel's law [16], and domains are visible only in dark field images.

The formation of IBs in wBN during hBN → wBN transformation plays an important role in the development of the wBN → zBN transition during the subsequent p, T treatment. Formally the wBN → zBN transition can proceed by ordered nucleation of intrinsic basal stacking faults connected with Shockley partial dislocations. The presence of IBs results in impeding of Shockley partials sliding. As a result the rearrangement of stacking sequence owing to intrinsic faults can start only after IB disappearance. We observed such processes in samples after heat treatment under static pressures when a decrease of IB density and nucleation of intrinsic faults took place (Fig. 4). So we can assume that IBs presence in wBN grains shifts the wBN → zBN transition to the higher temperature region.

Now we consider the puckering mechanism in the case of rBN → zBN transition. There is only one variant of rBN basal plane splitting (Fig. 5). Atom B1 must be displaced towards the atom N2 to create a tetrahedral bond. A displacement of B1 in opposite direction does not lead to tetrahedral coordination of atoms. So IB type defects can not form during puckering of rBN crystals. Nevertheless the real zBN structure formed by puckering is very imperfect (Fig. 6). We can not identify the type of faults by images on account of the high defect density. However, the strong diffusion streaks along the ⟨1 1 1⟩ directions seen in the SAD pattern of zBN

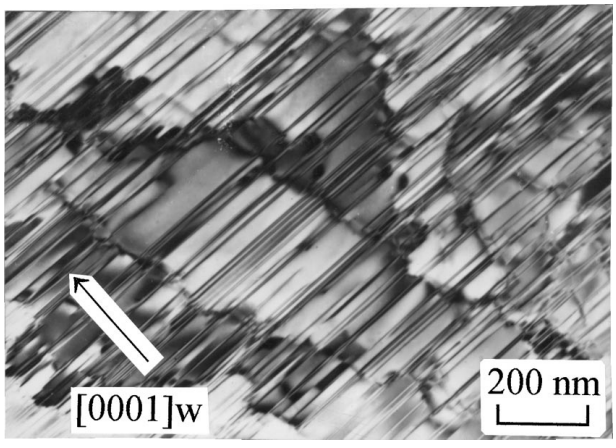

Figure 4 The microstructure of wBN after static treatment ($p = 7$ GPa, $T = 1300\,^{\circ}$C).

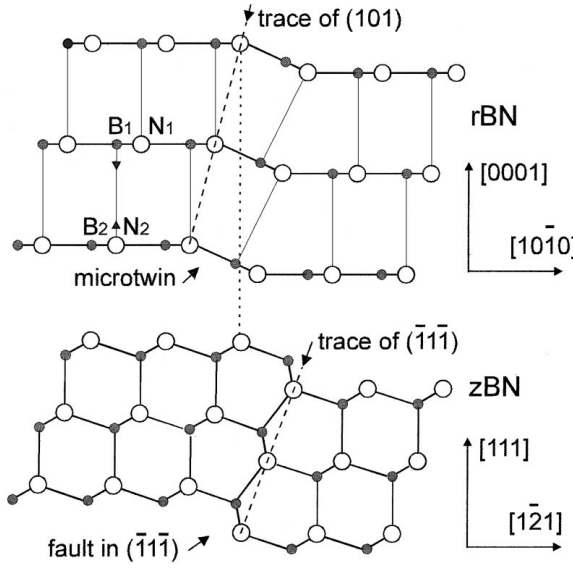

Figure 5 Scheme of rBN microtwin transformation into stacking fault of zBN.

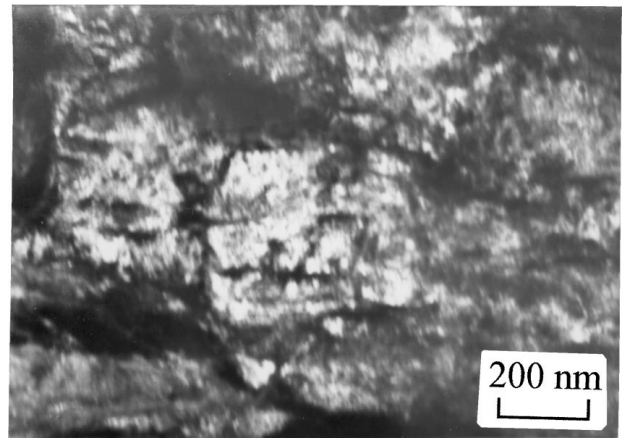

Figure 6 zBN microstructure formed during phase transformation, dark-field image, $g = 1\,1\,\bar{1}$.

(Fig. 1) point to high concentrations of stacking faults and microtwins in {1 1 1} planes. The defect concentration is especially high in the planes which are inclined to the (0 0 0 1) planes of the parent rBN phase. The formation of flat defects in these planes may be connected with two processes. The first process is microtwin formation in rBN under loading before the rBN → zBN transformation. Such twinning was observed in rBN experimentally [11]. The (1 0 1) planes of rBN twins are transformed during rBN → zBN transition to (1 1 1) planes of zBN, and flat defects in (1 0 1)r planes are transformed into flat defects in (1 1 1)z planes (Fig. 5). The second process is a plastic deformation of the new zBN phase. This deformation develops as a process of residual stress relaxation and it is connected with microtwin and deformation stacking fault formation.

4. Conclusion

The inversion boundaries in prismatic planes of wBN are appeared during hBN → wBN diffusionless transformation. Their generation is connected with the displacement of atoms of the same sort in neighbour nuclei

in opposite directions. The high density of inversion boundaries is indicative of a high nuclei density which are formed during transformation. This effect is due to the nonequlibrium conditions of martensitic type transitions.

The prismatic faults discovered in the wBN structure affect the wBN → zBN transition development. Perhaps their presence in wBN is one of the reasons which explain why the wBN → zBN diffusionless transition does not develop under shock compression.

The high density of faults in zBN is due to plastic deformation of parent and new phases which accompanies the rBN → zBN diffusionless transformation.

References

1. F. R. CORRIGAN and F. P. BUNDY, *Journal of Chemical Physics* **63**(9) (1975) 3812–3820.
2. P. K. LAM, R. M. WENTZCOVITCH and M. L. COHEN, *Materials Science Forum* **54/55** (1990) 165–192.
3. A. V. KURDYUMOV and A. N. PILYANKEVICH, "Phase Transformations in Carbon and Boron Nitride" (Kyev, Naukova dumka, 1979) p. 188, in Russian.
4. A. V. KURDYUMOV, N. F. OSTROVSKAYA, A. N. PILYANKEVICH and I. N. FRANCEVICH, *Dokl. Acad. Nauk USSR* **215**(4) (1974) 836–838, in Russian.
5. A. V. KURDYUMOV, V. G. MALOGOLOVEC, N. V. NOVIKOV *et al.*, "Polimorfic Modifications of Carbon and Boron Nitride" (Metallurgiya, Moscow, 1994) p. 318, in Russian.
6. T. SATO, I. ISHII and N. SETAKA, *Journal Amer. Ceram. Soc.* **65**(10) (1982) 162–167.
7. A. V. KURDYUMOV, N. F. OSTROVSKAYA, A. N. PILYANKEVICH *et al.*, *Dokl. Acad. Nauk USSR* **209**(5) (1973) 1081–1083, in Russian.
8. A. V. KURDYUMOV, *Powder Metallurgy* **12** (1975) 69–73, in Russian.
9. A. V. KURDYUMOV and V. A. PILIPENKO, *Dokl. Acad. Nauk USSR* **244**(2) (1979) 348–351, in Russian.
10. N. F. BOROVIKOV, A. S. GOLUBEV and V. G. KURDYUMOV, *Izvestiya Acad. Nauk USSR*, Neorg. Materiali, **19**(12) (1983) 2001–2005.
11. V. F. BRITUN, A. V. KURDYUMOV and I. A. PETRUSHA, *Journal of Materials Science* **28**(24) (1993) 6574–6581.
12. A. A. DERIBAS, "High Pressure Science and Technology," in Proceed XI AIRAPT Int. Conf. (Kiev, Naukova Dumka, 1989) Vol. 4, pp. 137–149.
13. H. IWANOGA, K. SUZUKI and S. TAKEUCHI, *Phil. Mag.* **34**(2) (1976) 291–298.
14. C. M. DRUM, *Phil. Mag.* **11**(110) (1965) 313–319.
15. L. T. CHADDERTON, A. G. FITZGERALD and A. D. IOFFE, *Phil. Mag.* **8**(85) (1963) 167–173.
16. S. AMELINCKX and J. VAN LANDUYT, "Contrast Effects at the Planar Interfaces, in Electron Microscopy in Mineralogy," edited by H. R. Wenk (Springer-Verlag Berlin, Heidlderg, New York, 1976) pp. 76–116.
17. P. B. HIRSCH, A. HOWIE, R. B. NICHOLSON, D. W. PASHLEY and M. J. WHELAN, "Electron Microscopy of Thin Crystals" (Butterworths, London, 1965).

Received 11 July 1996
and accepted 27 April 1999